BRAIN COMMUNICATIONS

Novel strain analysis informs about injury susceptibility of the corpus callosum to repeated impacts

Allen A. Champagne,[1] Emile Peponoulas,[1] Itamar Terem,[2] Andrew Ross,[3] Maryam Tayebi,[4] Yining Chen,[1] Nicole S. Coverdale,[1] Poul M. F. Nielsen,[4,5] Alan Wang,[4] Vickie Shim,[4] Samantha J. Holdsworth[6] and Douglas J. Cook[1,7]

Increasing evidence for the cumulative effects of head trauma on structural integrity of the brain has emphasized the need to understand the relationship between tissue mechanic properties and injury susceptibility. Here, diffusion tensor imaging, helmet accelerometers and amplified magnetic resonance imaging were combined to gather insight about the region-specific vulnerability of the corpus callosum to microstructural changes in white-matter integrity upon exposure to sub-concussive impacts. A total of 33 male Canadian football players ($mean_{age} = 20.3 \pm 1.4$ years) were assessed at three time points during a football season (baseline pre-season, mid-season and post-season). The athletes were split into a *LOW* ($N = 16$) and *HIGH* ($N = 17$) exposure group based on the frequency of sub-concussive impacts sustained on a per-session basis, measured using the helmet-mounted accelerometers. Longitudinal decreases in fractional anisotropy were observed in anterior and posterior regions of the corpus callosum (average cluster size $= 40.0 \pm 4.4$ voxels; $P < 0.05$, corrected) for athletes from the *HIGH* exposure group. These results suggest that the white-matter tract may be vulnerable to repetitive sub-concussive collisions sustained over the course of a football season. Using these findings as a basis for further investigation, a novel exploratory analysis of strain derived from sub-voxel motion of brain tissues in response to cardiac impulses was developed using amplified magnetic resonance imaging. This approach revealed specific differences in strain (and thus possibly stiffness) along the white-matter tract ($P < 0.0001$) suggesting a possible signature relationship between changes in white-matter integrity and tissue mechanical properties. In light of these findings, additional information about the viscoelastic behaviour of white-matter tissues may be imperative in elucidating the mechanisms responsible for region-specific differences in injury susceptibility observed, for instance, through changes in microstructural integrity following exposure to sub-concussive head impacts.

1 Centre for Neuroscience Studies, Room 260, Queen's University, Kingston, ON K7L 3N6, Canada
2 Department of Electrical Engineering, Stanford University, 350 Serra Mall, Stanford, CA, USA
3 Performance Phenomics, Toronto, ON, Canada
4 Auckland Bioengineering Institute, University of Auckland, Auckland Bioengineering House, L6, 70 Symonds Street, Auckland 1010, New Zealand
5 Department of Engineering Science, Faculty of Engineering, University of Auckland, Auckland 1010, New Zealand
6 Department of Anatomy and Medical Imaging & Centre for Brain Research, Faculty of Medical and Health Sciences, University of Auckland, Auckland 1023, New Zealand
7 Department of Surgery, Queen's University, Kingston, ON, Canada

Correspondence to: Douglas J. Cook
Department of Surgery
Queen's University
Room 232, 18 Stuart St.
Kingston, ON K7L 3N6, Canada
E-mail: dj.cook@queensu.ca

Received July 01, 2019. Revised August 15, 2019. Accepted August 21, 2019. Advance Access publication October 4, 2019

Keywords: sub-concussive impacts; amplified magnetic resonance imaging; diffusion tensor imaging; helmet accelerometers; tissue biomechanics

Abbreviations: λmax = maximum principal strain; aMRI = amplified magnetic resonance imaging; CC = corpus callosum; DTI = diffusion tensor imaging; FA = fractional anisotropy; GFT = gForce tracker; MRI = magnetic resonance imaging; ROI = region of interest; WM = white matter

Graphical Abstract

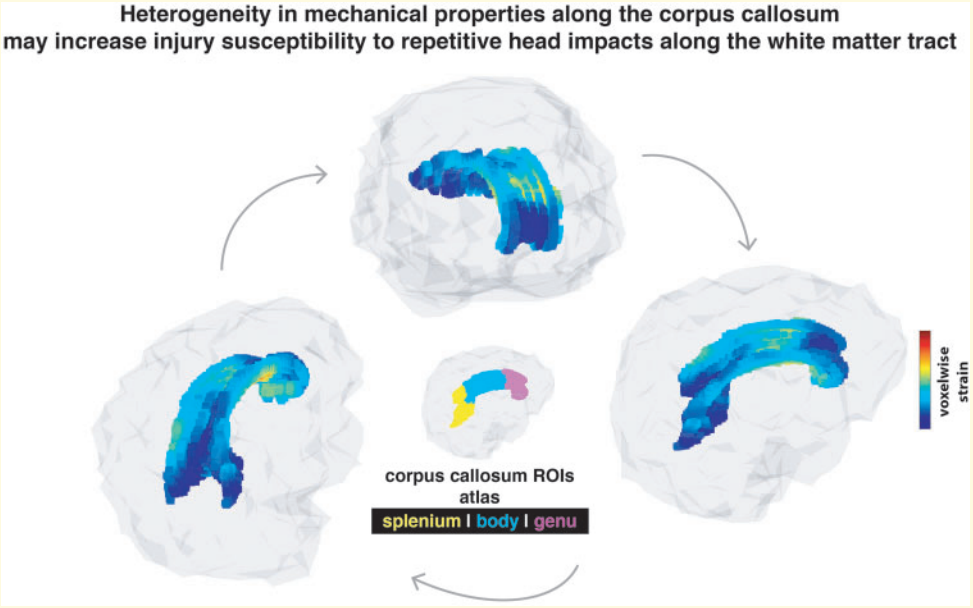

Introduction

A growing body of literature has raised concerns that repeated exposure to sub-concussive impacts to the head may increase the risks for short- and long-term changes in structural imaging biomarkers (Gajawelli *et al.*, 2013; Mcallister *et al.*, 2013; Chun *et al.*, 2015; Finn *et al.*, 2015; Churchill *et al.*, 2017). A sub-concussive collision is defined as a direct or indirect impact to the head during which mechanical forces transferred to the brain may alter axonal integrity without the presence of acute clinical or behavioural symptoms. This is in accordance with evolving theories that long-term exposure to such impacts may be associated with neurocognitive impairments (Hart *et al.*, 2013; Stamm *et al.*, 2015; McAllister and McCrea, 2017; Cookinham and Swank, 2018) and possible increased likelihood for early development of neurodegenerative pathologies (Baugh *et al.*, 2012). Although this remains a topic of debate (Asken *et al.*, 2017; Deshpande *et al.*, 2017; Broglio *et al.*, 2018; Caccese *et al.*, 2019), such evidence has motivated the need to uncover mechanisms relating repeated exposure to head impacts and changes in brain structure in order to improve the brain health of athletes.

Diffusion tensor imaging (DTI) has emerged as a promising magnetic resonance imaging (MRI) technique to expose changes in white matter (WM) architecture, following participation in contact sports (Gajawelli *et al.*, 2013; Mcallister *et al.*, 2013; Chun *et al.*, 2015; Finn *et al.*, 2015; Churchill *et al.*, 2017). Using DTI, a voxel-wise diffusion tensor can be estimated, from which information about dominant fibre direction and microstructural integrity (Basser *et al.*, 1994) can then be inferred to gather insight about the effects of repeated head impacts on brain structure over time. One DTI parameter of particular interest is fractional anisotropy (FA), which is primarily influenced by the integrity of the axonal membrane and the degree of myelination (Beaulieu, 2002; Zhang *et al.*, 2012).

In recent years, advances in computational modelling of head injuries have identified the corpus callosum (CC) as a fibre tract with high injury susceptibility (McAllister *et al.*, 2012; Stamm *et al.*, 2015; Hernandez *et al.*, 2019). As the largest commissural fibre tract in the brain, the density and fibre orientation of the CC appear to make this WM tract more vulnerable to diffuse axonal injury (Johnson *et al.*, 2012; McAllister *et al.*, 2012; Beckwith *et al.*, 2018; Hernandez *et al.*, 2019), due to the increased shear forces transferred locally, upon exposure to external acceleration/deceleration forces. Preliminary evidence from impact biomechanics (McAllister *et al.*, 2012; Hernandez *et al.*, 2019) suggests that differences in sub-structures within the anatomy of the CC, along with heterogeneity in the deformation fields induced from

mechanical loading, may contribute to the increased susceptibility of the CC for changes in WM integrity. Despite these findings however, research combining both DTI and *in vivo* measurements of tissue material properties is currently limited, which has constrained our understanding of the relationship between changes in tissue integrity and geometry following exposure to repeated head impacts.

The brain's tolerance to deformation upon exposure to loading forces is a function of the mechanical properties that make-up its tissues, as well as the kinetic parameters that characterize the impacts sustained over time (i.e. direction, magnitude, frequency; Browne *et al.*, 2011; Eucker *et al.*, 2011; Weaver *et al.*, 2012). Evidence from magnetic resonance elastography suggests that cerebral tissues vary in orders of magnitude with respect to stiffness (measured in kPa; Murphy *et al.*, 2017), which provides insight about a material's ability to resist, and deform, under a certain load. Stiffness estimates are influenced by the mechanical and structural properties of the biological tissues, the dynamic interactions between cellular and extracellular compartments and the direction of the load (reviewed in Murphy *et al.*, 2017). According to Young's modulus (Jeppesen, 2005), stiffness is inversely related to strain by way of the relationship between the change in shape of a specific structure, and the stress applied from an elastic (recoverable) load. Following this principle, stiffer WM tracts (e.g. high Young's modulus) may undergo smaller strain (deformation gradients) upon exposure to mechanical stress of a given magnitude, which may affect the propagation of shear waves along the fibres. Thus, additional information about the viscoelastic behaviour of WM tissues may be imperative for elucidating the mechanisms responsible for region-specific differences in injury susceptibility observed, for instance, through changes in microstructural integrity along the CC.

Recent development of movement-based imaging modalities such as DENSE-MRI (Aletras *et al.*, 1999; Adams *et al.*, 2019) and amplified magnetic resonance imaging (aMRI) has shown promising results for studying the complex motions of the brain, based on physiological dynamics (Holdsworth *et al.*, 2016; Terem *et al.*, 2018). aMRI uses the periodic cardiac-induced blood pulsation as a loading force to visualize and quantify sub-voxel displacement of brain tissues. Post-processing magnification algorithms of aMRI integrate methods such as Eulerian Video Magnification (Holdsworth *et al.*, 2016) and phase-based video motion processing (Terem *et al.*, 2018), with the latter thought to be less prone to noise and less sensitive to non-motion induced voxel intensity changes. Recently, aMRI has been used to characterize minute differences in brain movement as a result of Chiari I malformation (Terem *et al.*, 2018), suggesting that novel harmonic-based pre-processing algorithms may be useful in assessing tissue material properties in clinical populations.

In this study, we combined DTI, aMRI and helmet accelerometers to gather insight about the region-specific vulnerability of the CC to microstructural changes in integrity, upon exposure to repeated sub-concussive impacts. First, a longitudinal imaging design with DTI was used to characterize changes in FA within the CC, based on differences in frequency of sub-concussive collisions, throughout a season of Canadian collegiate football. It was hypothesized that changes in FA would be specific to athletes who sustain more frequent impacts to the head on a per-session basis, given the repetitive nature of the loading mechanisms on structures of the CC. Using these findings as a basis for further investigation, we then acquired cross-sectional neuroimaging datasets including both DTI and aMRI to develop a novel post-processing analysis of tissue strain. This exploratory approach was implemented to explore whether differences in strain measurements may provide a mechanistic explanation for the differences in injury susceptibility of the WM tract.

Materials and methods

Subjects and ethical approval

The protocol used in this work was approved by the Queen's University Health Sciences Research Ethics Board (Kingston, ON, Canada) and informed consent was obtained for all participants according to the Declaration of Helsinki (World Medical Association, 2001).

Two distinct datasets were acquired for the purpose of this study (Fig. 1). First, to explore the effect of sub-concussive impacts on the integrity of the CC, a total of 33 male Canadian football players (Table 1) were enrolled in the longitudinal neuroimaging protocol (Fig. 1; blue). Structural images acquired included a high-resolution anatomical image and DTI only, as part of a larger MRI protocol. The first imaging time point was completed prior to the pre-season training camp, within 2 months before the first contact practice ('*PRE*'), to serve as a baseline for the DTI measurements. Of those 33 athletes, two sustained a sport-related concussion, while two suffered musculoskeletal season-ending injuries during training camp. One subject decided to remove himself from the study. Thus, a total of 28 players returned for imaging post-training camp ('*PTC*'), scheduled following the 14-day training camp period and the first two games of the season. One imaging dataset was removed from this time point due to corruption in the acquired file, giving a total of 27 valid *PTC* datasets. Finally, a total of 24 players successfully completed the final imaging time point, 1 month following the last competitive game of the season ('*POST*'). The *POST* data were collected because athletes do not engage in contact activity following the last game which we hypothesized could allow for changes in imaging markers to return towards baseline. Four athletes from the *PTC* time point did not complete the *POST* neuroimaging due to sport-related concussions ($N = 2$) and season-ending injuries ($N = 2$). One dataset

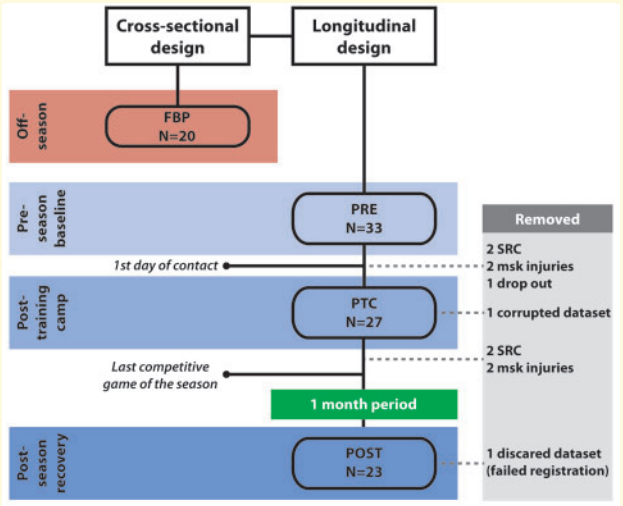

Figure 1 Schematic of the data collection design. Data acquired longitudinally over the course of the season (blue) included a 3D T_1-weighted anatomical scan and DTI only. Data collected for the cross-sectional analysis of strain along the CC (red) included a 3D T_1-weighted anatomical scan, DTI and aMRI. Removed subjects from the longitudinal study along the way are shown in grey. msk = musculoskeletal, SRC = sport-related concussion.

from the *POST* time point was removed due to failed registration in standard space caused by distortion in the image (Fig. 1).

The second arm of this study (Fig. 1; red) was designed to explore the region-specific distribution of strain patterns along the CC using a novel analytical approach from aMRI. Here, a cross-sectional sub-sample of 20 athletes were recruited for imaging in the off-season (Table 1), of which seven had also participated in the longitudinal study design.

Characterizing player-specific exposure to sub-concussive impacts

The football helmets of athletes followed longitudinally throughout the season were mounted with gForce tracker accelerometers (gForce Tracker; Hardware version GFT3S ver4.0, Artaflex Inc., Markham, ON, Canada), in order to characterize exposure to sub-concussive impacts on a per-session basis. This gForce tracker hardware has been validated in laboratory settings to provide supporting evidence that the system is appropriate for monitoring head impacts in football helmets (Campbell *et al.*, 2016). gForce tracker sensors were attached between the upper left paddings of the helmets and set to a minimum peak linear acceleration threshold equal to 15 g (Campbell *et al.*, 2016; Champagne *et al.*, 2019).

A total of five impact locations (i.e. 'front', 'top', 'right', 'left' and 'back') were categorized based on information collected from the sensor about the elevation and azimuth angle, similar to Mihalik *et al.* (2007). Additionally, peak linear acceleration (g) and rotational velocity (°/s) were collected for each impact above the triggering threshold.

Magnetic resonance imaging acquisition

All images were acquired on a Siemens 3.0 T Magnetom Tim Trio system using a 32-channel receiver head coil. A T_1-weighted structural image of the whole brain was acquired using a magnetization-prepared rapid gradient echo pulse sequence and the following parameters: repetition time = 1760 ms, echo time = 2.2 ms, inversion time- = 900 ms, voxel size = 1 mm isotropic, flip angle = 9°, bandwidth = 200 Hz/Px, for a total scan time of 7 min and 32 s.

Diffusion-weighted images were acquired with 30 phase-encoding directions (b-value = 1000 s/mm^2) and the following parameters: repetition time = 7800 ms, echo time- = 95 ms, field of view = 256 mm, 60 axial slices, 128 × 128 acquisition matrix, slice thickness = 2.0 mm, voxel size = 2 mm isotropic, echo spacing = 0.84 ms, GRAPPA parallel imaging (acceleration factor = 3), bandwidth = 1396 Hz/Px. Three additional non-diffusion-weighted reference volumes (b_0 = 0 s/mm^2) were acquired, for a total of four baseline images, including two with the phase-encoding polarity reversed (i.e. posterior–anterior).

The aMRI acquisition uses the cardiac-gated balanced steady-state free precession sequence (Holdsworth *et al.*, 2016; Terem *et al.*, 2018) to collect a short MRI 'movie' of the brain that is normalized to the heartbeat, followed by the amplification of the sub-voxel motion using a video-processing technology (Wadhwa *et al.*, 2013). The balanced steady-state free precession sequence used here was a 2D multi-slice acquisition, acquired over different phases of the cardiac cycle (covering a single heartbeat) using the cardiac-gated MRI pulsometer as the triggering mechanism. Thus, it is assumed that the temporal cycle for each slice, which corresponds to the heart harmonics, is aligned with the temporal component of the heartbeat frequency. 2D sagittal slices of the whole brain were acquired in an interleaved fashion, using the following imaging parameters: matrix size = 192 × 192, flip angle = 45°, repetition time/echo time = 40.92/1.51 ms, receiver bandwidth = 965 Hz/pixel, voxel size = 1.3 × 1.3 mm, slice thickness = 5.0 mm, field of view = 256 × 256 mm, GRAPPA parallel imaging (acceleration factor = 2), number of segments = 12, number of calculated cardiac phases = 85. A total of 27 sagittal slices were acquired for a total scan time of ~5 min, depending on the participant's heart rate.

Data pre-processing

Diffusion tensor imaging

Diffusion tensor images were processed using the FMRIB Diffusion Toolbox as part of the FSL (FMRIB's Software

Table 1 Subject demographics separated by study design

	Longitudinal design (*N* = 33)	Cross-sectional design (*N* = 20)
Structural imaging acquired	T_1-weighted anatomical scan, DTI	T_1-weighted anatomical scan, DTI and aMRI
Age (years)	20.3 ± 1.4	19.6 ± 1.3
Height (cm)	184.0 ± 5.5	185.1 ± 4.9
Weight (kg)	94.0 ± 10.2	97.7 ± 13.9
Number of prior concussions (*N*)	0.8 ± 1.0 (range: 0–4)	0.6 ± 1.0 (range: 0–2)
Time since injury (years)	4.8 ± 3.0 (range: N/A–9)	3.2 ± 2.0 (range: N/A–6)
Position (*N*)	DB (7)	
	DL (4)	
	FB (2)	
	K (1)	DB (6)
	LB (8)	DL (8)
	QB (2)	LB (5)
	RB (1)	RB (1)
	S (2)	S (1)
	TE (2)	
	WR (4)	

Values are mean ± standard deviation.
aMRI = amplified magnetic resonance imaging; DB = defensive back; DL = defensive lineman; DTI = diffusion tensor imaging; FB = full back; K = kicker; LB = linebacker; N/A = not applicable; QB = quarterback; RB = running back; S = safety; TE = tight-end; WR = wide-receiver.

Library) software package (http://fsl.fmrib.ox.ac.uk/fsl/; Smith *et al.*, 2004; Woolrich *et al.*, 2009; Jenkinson *et al.*, 2012). Initial pre-processing steps included averaging the four b_0 sets, eddy current and motion correction, and exclusion of non-brain tissues. To correct for eddy currents, the susceptibility-induced off-resonance field from all paired b_0 volumes was estimated using a method described in Andersson *et al.* (2003) and implemented in FSL (Smith *et al.*, 2004) through the 'topup' and 'eddy' functions. Once corrected, the diffusion data and brain mask output were used to calculate the 3×3 diffusion tensor parameters in each brain voxel using *DTIFIT*. The three eigenvectors were then used to compute the FA map for each subject, as an index of microstructural integrity within the CC (Basser *et al.*, 1994). The primary eigenvalue maps, also known as axial diffusivity, were also used to extract the principal fibre direction along the CC for comparison with the aMRI-based strain maps (discussed below).

Amplified magnetic resonance imaging

The aMRI movie was amplified using an algorithm developed in-house using MATLAB (2018b, The MathWorks, Inc., Massachusetts, USA) scripts, in order to reveal the sub-voxel motion of the CC (Terem *et al.*, 2018). The algorithm assumes that changes in the signal intensity of the volumes acquired over time is minimal, meaning that all motion driven from the cardiac impulse function is sub-voxel. This way, the amplification algorithm can be used to magnify the temporal changes occurring at a fixed location and over a specific range of user-selected frequencies.

Using the aMRI algorithm, discussed in more depth in Terem *et al.* (2018), each frame was first decomposed into scale and orientation components, using a steerable pyramid (Fig. 2A). The steerable pyramid is an image decomposition method that uses directional derivative operators as a basis function. The functions are not spatial alias, and as a result, complex-value coefficients are computed which reflect the signal amplitude and phase. The amplification is thus achieved by varying the phases of the complex-values coefficients, which correspond to a translation in the image domain via the Fourier shift theorem. Following image decomposition, the temporal phases of each pixel were bandpass filtered to the fundamental frequency of the motion (1 Hz; Fig. 2B) and multiplied by a user pre-set amplification factor which allowed enough amplification of the sub-voxel motion without introducing significant artefacts (Fig. 2C). Finally, the pre-processed phase was added back to the original phase value, in order to reconstruct each frame (Fig. 2D) and thereby create the amplified movie of the brain motion normalized to the heartbeat.

Principal maximum strain mapping from the amplified sub-voxel motion

The amplification algorithm outputs a 4D movie (Fig. 3A) where each frame, for every 2D slice, is converted into a NIFTI image. For each frame, the interleaved slices were then aligned using 2D rigid affine linear registration (Fig. 3B; *FLIRT*; Jenkinson and Smith, 2001; Jenkinson *et al.*, 2002), and concatenated in the third dimension to reconstruct the amplified volumes in 3D over time (Fig. 3C). This approach takes advantage of the major non-brain rigid bodies that are not affected by the physiological pulsations, in order to align the slices together for each frame. This approach also leverages the fact that each 'movie' slice is acquired based on the cardiac-gating mechanism. All slices are thus normalized and amplified on the same temporal frequency of the heartbeat.

Once reconstructed, the 3D volumes were concatenated in the fourth dimension and averaged over time for extraction of non-brain tissues using *BET* (Jenkinson *et al.*, 2012), in order to restrict the following pre-processing steps to brain tissues only (Fig. 3C). To quantify the frame-to-frame displacement from the amplified sub-voxel motion, each reconstructed 3D amplified volume was warped to the preceding frame (Fig. 3D) using non-linear imaging registration (*FNIRT*; Andersson *et al.*, 2007). This process outputs a 4D file containing the warp-fields in all three axes (*x*-, *y*- and *z*-directions), which can then be used to reconstruct the strain tensor (explained below), and compute voxelwise principal maximum strain maps. No rigid or affine initialization was used for

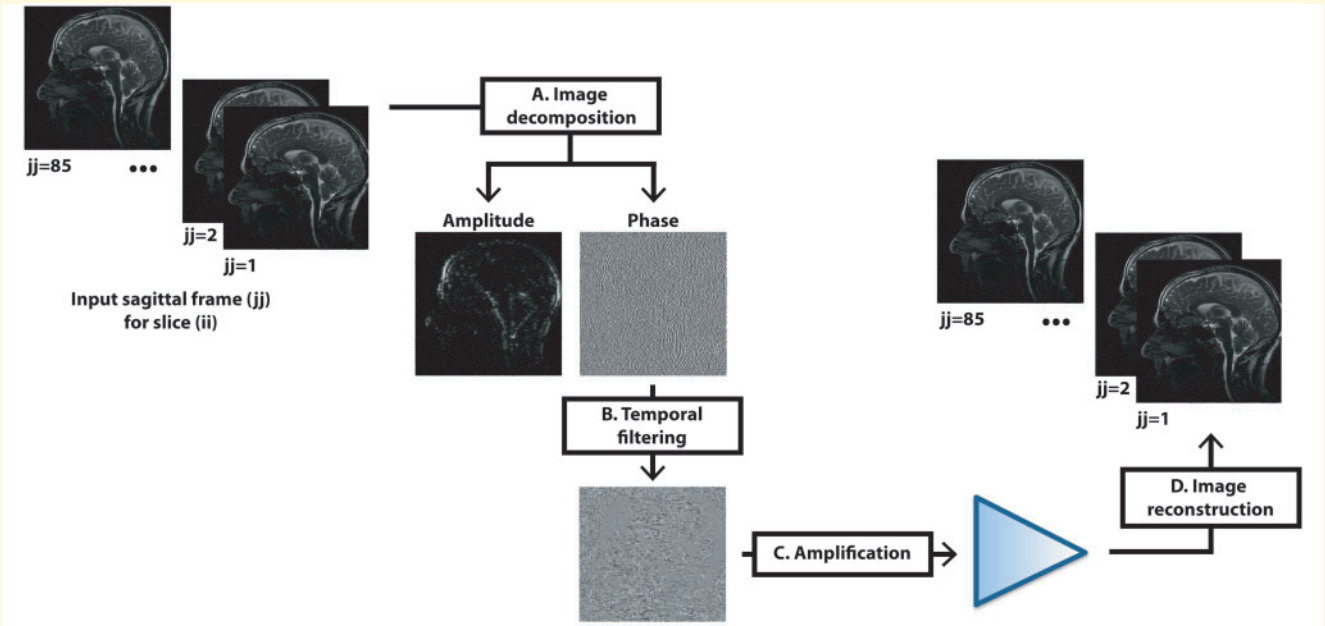

Figure 2 Amplified magnetic resonance imaging pre-processing workflow for the amplification of sub-voxel brain motion.

analysing the interframe similarity over time from the 3D amplified volumes.

Following image pre-processing, warp fields were imported back into the MATLAB interface to compute the voxelwise strain tensors. First, the displacement in each direction was averaged over time (Fig. 3E) to create a voxelwise mean displacement map along each axis. Then, directional gradients of the 3D image were computed for each direction using partial derivatives (Fig. 3F), in order to create deformation maps along the x (μ_x, μ_y, μ_z), y (ν_x, ν_y, ν_z) and z (ω_x, ω_y, ω_z) axes. These maps were then used to compute the normal (ϵ_{xx}, ϵ_{yy}, ϵ_{zz}) and shear strain (ϵ_{xy}, ϵ_{xz}, ϵ_{yz}) parameters, which were transposed to fill-in the 3D strain matrix [Eq. (1)]:

$$\text{Voxelwise tensor} = \begin{bmatrix} \epsilon_{xx} & \epsilon_{xy} & \epsilon_{xz} \\ \epsilon_{yx} & \epsilon_{yy} & \epsilon_{yz} \\ \epsilon_{zx} & \epsilon_{zy} & \epsilon_{zz} \end{bmatrix} \quad (1)$$

assuming symmetry within the geometry of the tensor (i.e. $\epsilon_{xy} = \epsilon_{yx}$). From here, the diagonal matrix of the tensor was solved to compute the maximum eigenvalue (Fig. 3G) and its matching eigenvector, which provided information about the maximum principal strain (maximum principal strain $= \lambda_{max} =$ principal eigenvalue) and the primary direction of the strain, on a voxel-per-voxel basis.

Statistical analysis

Longitudinal analysis of microstructural integrity within the corpus callosum based on exposure to head impacts

In order to explore the effects of exposure on WM integrity of the CC over time, athletes followed longitudinally were grouped into a 'LOW' or 'HIGH' exposure group based on the averaged count of head impacts sustained per-session. Impact frequency was normalized per-session in order to characterize an exposure profile for each athlete, while accounting for missed sessions due to technical difficulties with the sensors, which would inherently bias a cumulative sum of all recorded impacts. Participants were separated based on the group median and assigned to the 'LOW' (below the median) or 'HIGH' (above the median) exposure group. In this analysis, the *LOW* subjects served as the control group in order to account for possible changes in FA over time, unrelated to greater exposure to head impacts.

Prior to the voxelwise analysis of the CC, FA maps were warped into 1 mm Montréal Neurological Institute space using linear (Jenkinson and Smith, 2001; Jenkinson *et al.*, 2002) and non-linear (Andersson *et al.*, 2007) transformation that registered native images to Montréal Neurological Institute space, via the anatomical scan. Montréal Neurological Institute-aligned FA maps were then assessed for changes over time using a two by three factors mixed ANOVA. Analysis of functional neuroimages (AFNI)'s *3dLME* function (Cox, 1996) was used to conduct the voxelwise analysis, in order to include all valid datasets from the three time points (within-subject; *PRE*, *PTC*, *POST*), and the exposure group factor (between-subject; *LOW*, *HIGH*), while accounting for missing data throughout the season related to injuries. Subjects were modelled as a random effect. This analysis was restricted to the CC only, given the possible vulnerability of the tract to repeated head impacts, as highlighted above. Statistical significance from the voxelwise analysis was determined using a parameter-specific cluster size

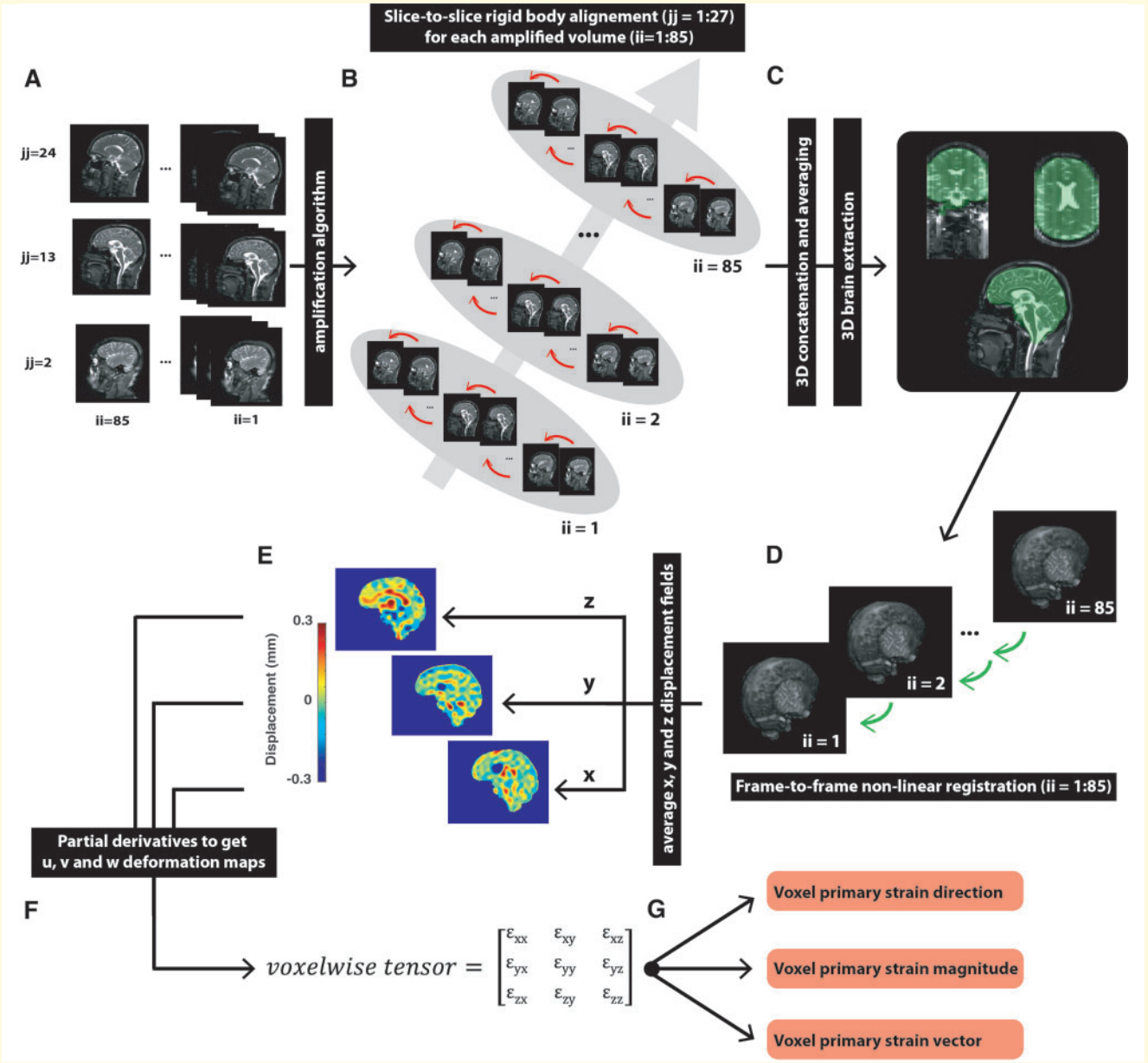

Figure 3 Computation of the voxelwise strain parameter map derived from the sub-voxel motion in aMRI. (**A**) Amplification of sub-voxel motion using aMRI. (**B**) For each volume (jj) over time, 2D sagittal slices (ii) were realigned using rigid-body linear registration (6 dof) to reconstruct the 3D volume (**C**), and extract brain tissues. (**D**) Subsequent frames (e.g. frame 2 to frame 1, frame 3 to frame 2, and so on) were warped to one another to quantify the sub-voxel motion in all orthogonal directions (i.e. *x, y, z*) over time. Mean displacement fields (**E**) in each direction were then used to compute deformation maps using partial derivatives (**F**), and then solve the strain tensor on a voxel-per-voxel basis (**G**).

(corrected for family-wise error at $P < 0.05$) computed using Monte Carlo simulations (10 000 iterations) in AFNI's *3dFWHMx* (with spatial AutoCorrelation) and *3dClustSim* (Cox, 1996; Cox *et al.*, 2017). Significant clusters for the interaction between time and exposure were then combined and converted to a binary mask to extract mean regional FA in each subject, at all time points, for *post hoc* analyses. These were conducted in IBM SPSS statistics (version 24.0, SPSS Inc., Chicago, IL, USA) using pairwise comparisons between the time points (i.e. *PRE* versus *PTC*, *PRE* versus *POST* and *PTC* versus *POST*).

Cross-sectional analysis of the maximum principal strain along the corpus callosum

Following co-registration and alignment between the aMRI and anatomical images (Fig. 4), segmented region of interests (ROIs) of the CC (i.e. genu, body and splenium) were extracted using the John Hopkins University DTI-based

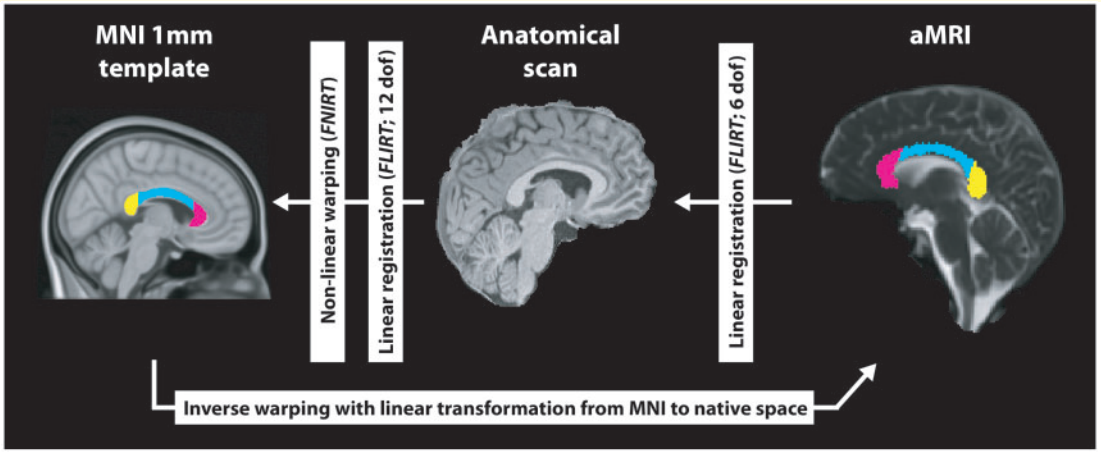

Figure 4 Normalization and segmentation of the CC region-of-interest in native space. The genu (pink), body (blue) and splenium (yellow) of the CC were re-sampled in native space with the aMRI baseline scan via reversed transformation matrices, and warp fields, that align the native aMRI coordinates to the structural and Montréal Neurological Institute 1 mm template brain. These segmented regions were used to extract regional principal maximum strain (see Fig. 2) along the CC.

white-matter atlas (Ling and Rumpel, 2006; Wakana *et al.*, 2007; Hua *et al.*, 2008). ROIs were then warped back into native space using concatenated, and inversed, linear and non-linear transformations that registered anatomical images to standard template space (Fig. 4).

Once aligned, the low-resolution CC masks were used to extract λ_{max} from the aMRI-based strain maps, along with the primary strain tensor direction of the principal vector. Differences in regional distribution of the λ_{max} across the CC (i.e. genu versus body versus splenium) were assessed using a univariate ANOVA across all three regions. Statistical significance (set at $P < 0.05$) was determined using *post hoc* pairwise comparisons between each ROIs mean λ_{max} values (i.e. genu versus body, genu versus splenium and body versus splenium), to assess strain-based differences along the fibre tract. The same ROIs aligned in native DTI space were also used to extract the principal direction of the diffusion-based tensor, to explore whether fibre principal strain (from aMRI) and fibre principal direction (from DTI) were aligned.

Data availability

The data and scripts that support the findings of this study are available from the corresponding author, upon reasonable request.

Results

Data-informed grouping of participants based on helmet accelerometer data

Two groups [$N(LOW) = 16$; $N(HIGH) = 17$] were derived from the helmet impact kinematic data. An equal number of starter and back-up athletes were distributed across both the *LOW* ($count_{starters} = 9$, $count_{back\text{-}ups} = 8$) and *HIGH* ($count_{starters} = 8$, $count_{back\text{-}ups} = 8$) groups suggesting that opportunities for athletic exposure on the field based on starting status were relatively balanced between the groups (Supplementary Table 1). The median average frequency of head impacts per-session used to separate the participants was 9.3. In addition to differences in the number of sub-concussive impacts sustained on a per-session basis, larger mean linear acceleration ($P = 0.019$; Supplementary Table 2) and rotational velocity ($P = 0.002$; Supplementary Table 2), per-session, were documented for the *HIGH* group, compared to *LOW*. Finally, no significant difference in history of concussion was observed between the *LOW* and *HIGH* groups ($P = 0.745$).

Exposure-specific differences in white-matter integrity within the corpus callosum over time

Voxelwise analysis of the FA maps within the CC showed a significant interaction between time and exposure (Fig. 5) in three clusters within the WM tract (Supplementary Table 3), averaging in size at 40.0 ± 4.4 voxels. The significant clusters were distributed towards the anterior and posterior regions of the CC (Fig. 5A and B), within the genu ($N = 1$) and the splenium ($N = 2$). No significant differences surrounding the midsection of the CC were documented (Fig. 5A and B).

Post hoc analyses of the regional FA within the clusters for the main effect of time showed that the significant interaction was driven primarily by alterations in FA within the *HIGH* group (Fig. 5C; $F(2,22) = 32.60$, $P = 2.85 \times 10^{-7}$). Specifically, FA was decreased at the

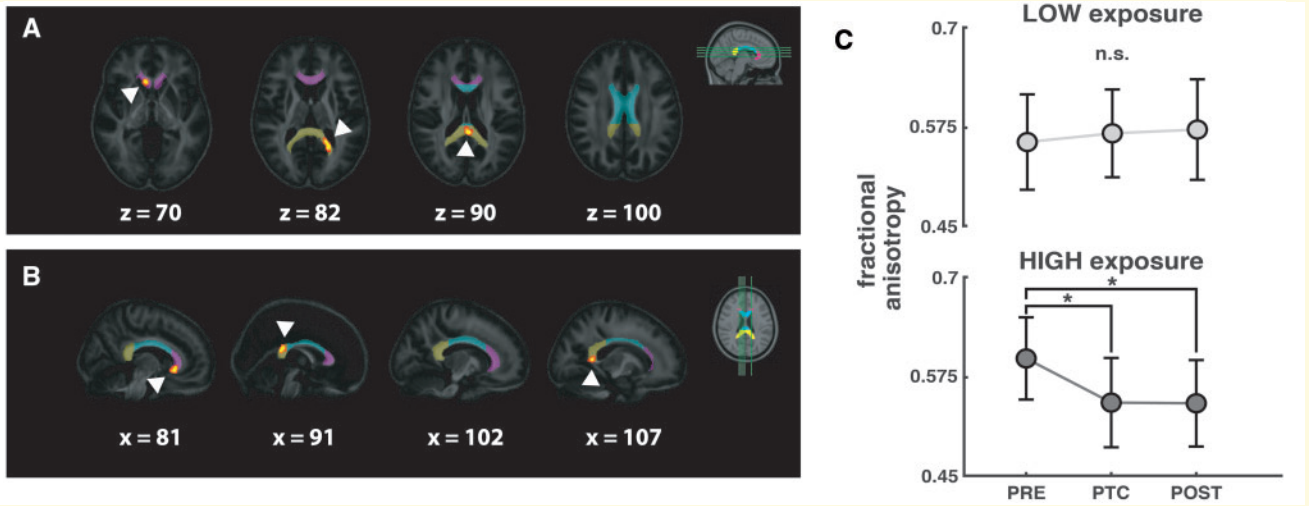

Figure 5 Significant results showing microstructural changes in white-matter integrity based on the interaction between time and exposure to repetitive head impacts. (**A** and **B**) The three significant clusters (see Supplementary Table 3; red-yellow) are overlaid over the group-mean FA map, along with the segmented CC (pink = genu, blue = body, yellow = splenium). These significant clusters show the spatial distribution of the microstructural changes in white matter along the CC determined using a voxelwise two (LOW, HIGH) by three (PRE, PTC, POST) factors mixed linear model to account for missing data throughout the season (see Fig. 1). Axial (**A**) and sagittal (**B**) slices are displayed in 1 mm Montréal Neurological Institute space. Clusters were inflated using *tbss_fill* for visual display. (**C**) Mean FA (± standard deviation) extracted for the entire significant region-of-interest highlighted in (**A** and **B**) are plotted to show that changes in microstructural integrity of the white-matter tract were specific to players who sustained a greater number of impacts per-session [*HIGH* group; $N_{PRE(HIGH)} = 17$, $N_{PTC(HIGH)} = 13$ and $N_{POST(HIGH)} = 10$], compared to the players from the *LOW* exposure group [$N_{PRE(LOW)} = 16$, $N_{PTC(LOW)} = 14$ and $N_{POST(LOW)} = 13$]. No significant (n.s.) changes in FA were recorded for the *LOW* group.

PTC ($P = 3.0 \times 10^{-6}$) and *POST* ($P = 1.0 \times 10^{-6}$) time points, compared to the *PRE* measurement. No statistical differences in FA were found between the *PTC* and *POST* time points ($P = 0.970$). Lastly, no significant effect of time across all time points was observed within the *LOW* exposure group [Fig. 5C; $F(2,25) = 0.818$, $P = 0.453$], and thus, no further *post hoc* analyses were conducted.

Region-specific differences in principal maximum strain along the corpus callosum

ROI-based analysis of the strain across the CC showed significant differences along the tract [$F(2) = 14.69$, $P = 7.0 \times 10^{-6}$; Table 2; Fig. 6A]. Specifically, higher λ_{max} was documented in the body of the CC, with respect to both the genu ($P = 3.23 \times 10^{-4}$) and the splenium ($P = 2.00 \times 10^{-6}$). No statistical difference in strain was observed between the genu and the splenium ($P = 0.165$).

Despite differences in the magnitude of the strain across the tract, all ROIs showed that the majority of primary strain-based tensors were aligned along the left-to-right axis of the head (Table 2; Fig. 6B), which runs parallel to the most common fibre direction within the CC (Table 2; Fig. 6C).

Discussion

Main findings

To the best of our knowledge, this study design is the first to combine helmet accelerometers, DTI and aMRI to expand our understanding of the relationship between repeated exposure to sub-concussive collisions and region-specific differences in injury susceptibility along the CC. Our findings provide robust evidence that microstructural changes in WM integrity may be specific to players sustaining a larger number of impacts to the head per-session, which emphasize the need to regulate exposure to contact during the season. Second, results from the exploratory arm of this study using aMRI introduce the possibility that differences in mechanical properties along the CC may expose anterior and posterior regions to greater structural changes in integrity over time, supporting a close relationship between fibre structure and tissue-based injury susceptibility.

Changes in white-matter integrity of the corpus callosum relating to higher exposure to sub-concussive head impacts

Decreases in FA within the CC were specific to players who sustained more sub-concussive head impacts per-session,

Table 2 Regional distribution of strain- and fibre-based parameters across the CC computed from aMRI and DTI maps

CC ROI	Principal maximum strain (λ_{max})	Primary maximum strain direction (% voxels in mask)	Primary diffusion-based fibre direction (% voxels in mask)
Genu	8.10 ± 1.98	L–R (64 ± 13%)	L–R (85 ± 4%)
Body	10.65 ± 2.81	L–R (54 ± 10%)	L–R (69 ± 5%)
Splenium	7.17 ± 1.19	L–R (49 ± 12%)	L–R (67 ± 8%)
P-value[a]	<0.0001*,***	N/A	N/A

Values are mean ± standard deviation.
[a]ROI strain was compared using a univariate ANOVA with location (i.e. genu, body, splenium) as the fixed factor. Pairwise comparisons were conducted upon statistical significance ($P < 0.05$). *,*** = indicates significant difference between the genu and body (*), or the body and splenium (***).
I–S = inferior to superior; L–R = left to right; N/A = not applicable; P–A = posterior to anterior; ROI = region-of-interest.

suggesting that changes in WM integrity along the CC may be possible during the season without a clinical diagnosis or symptomatic response associated with concussion. This is in line with findings from Bazarian *et al.* (2014) who showed no relationship between documented changes in WM integrity and clinical outcome measures studied up to 6 months following exposure to contact. Together, these findings suggest that changes in structural imaging markers from repeated sub-concussive impacts sustained over the course of a football season may be 'silent' in nature. The regional distribution of the significant clusters within the CC observed in this study (Fig. 5; Supplementary Table 3), along with the direction of the changes in FA, are also concordant with existing literature on repeated head trauma. In previous work with professional boxers (Chappell *et al.*, 2006; Zhang *et al.*, 2006; Herweh *et al.*, 2016), decreases in FA along the CC were documented compared to controls, suggesting that changes in microstructural integrity of the fibre tract may occur as a result of repeated diffuse axonal microinjuries. Changes in diffusion parameters within the sub-cortical and intra-hemispheric regions were also related to the number of fights (e.g. inverse relationship with FA; Herweh *et al.*, 2016) emphasizing a possible relationship between increased exposure to head impacts and changes in tissue integrity. This raises important questions about the long-term effects of such exposure, given existing reports of changes in FA and cognitive impairments in aging retired professional football players (Hart *et al.*, 2013). Decreases in FA may be interpreted as possible changes in the degree of myelination of the axons, or increases in water content from cellular inflammation processes recruited in response to the diffused axonal injury (Wilde *et al.*, 2008; Cubon *et al.*, 2011; Zhang *et al.*, 2012). These may be specific to the anterior and posterior regions of the CC due to differences in fibre composition (Aboitiz *et al.*, 1992), and/or heterogeneity in tissue mechanic properties (discussed next), along the WM tract.

Changes in FA along the CC reported in this study were specific to players within the *HIGH* exposure group only. These findings suggest that the frequency of impacts sustained on a per-session basis, as an index for exposure, can modulate the risk for changes in WM integrity. It is important to note that although differences in linear acceleration and rotational velocity were also found between the *HIGH* and *LOW* groups; these metrics are likely related to the frequency of impacts recorded per-session via the intrinsic characteristics that define an athlete's playing style on the football field (Schmidt *et al.*, 2016; Kuriyama *et al.*, 2017). Specifically, players that engage in more contact with their helmet may also have a unique style of play that pre-dispose them to larger kinematic measurements, and thereby possibly compromise the structural integrity of the CC. These findings are similar to previous literature (Bazarian *et al.*, 2014) showing that changes in FA between *pre-* and *post*-season timepoints (i.e. at the end of the season and after 6 months of rest) were related to several impact kinematic measurements, indicating that greater helmet impact exposure may be associated with more changes in WM integrity. Decreases in FA for the *HIGH* players in this study were specific to the *PTC* and *POST* time points, compared to the *PRE*-season measurements. The timeline for these changes in FA suggests that alterations in WM structural integrity may occur during the season upon participation in contact activities, and persist 1 month after no exposure to contact, which is in agreement with previous literature (Bazarian *et al.*, 2014).

Differences in injury susceptibility due to possible heterogeneity in mechanic properties along the corpus callosum

This article is the first to incorporate knowledge from aMRI to gather insight about the potential injury susceptibility of the CC with respect to repetitive sub-concussive loading events in football. Differences in λ_{max} measurements between the body and the anterior and posterior regions of the CC were documented. These were co-localized with the spatial distribution of the changes in FA observed in athletes sustaining a higher number of sub-concussive impacts per-session. Specifically, lower mean λ_{max} was found within the genu and the splenium, compared to the body. Based on Young's modulus (Jeppesen, 2005), a lower strain in the extremities of the CC could possibly indicate a higher tissue stiffness, and thus more rigid fibre structures. These regions may therefore be more vulnerable to repetitive mechanical loading from external forces applied to the brain (i.e. sub-concussive impacts). Higher stiffness upon exposure to loading mechanisms may affect the way shear wave forces are propagated through the WM fibres, which in turn, could result in greater

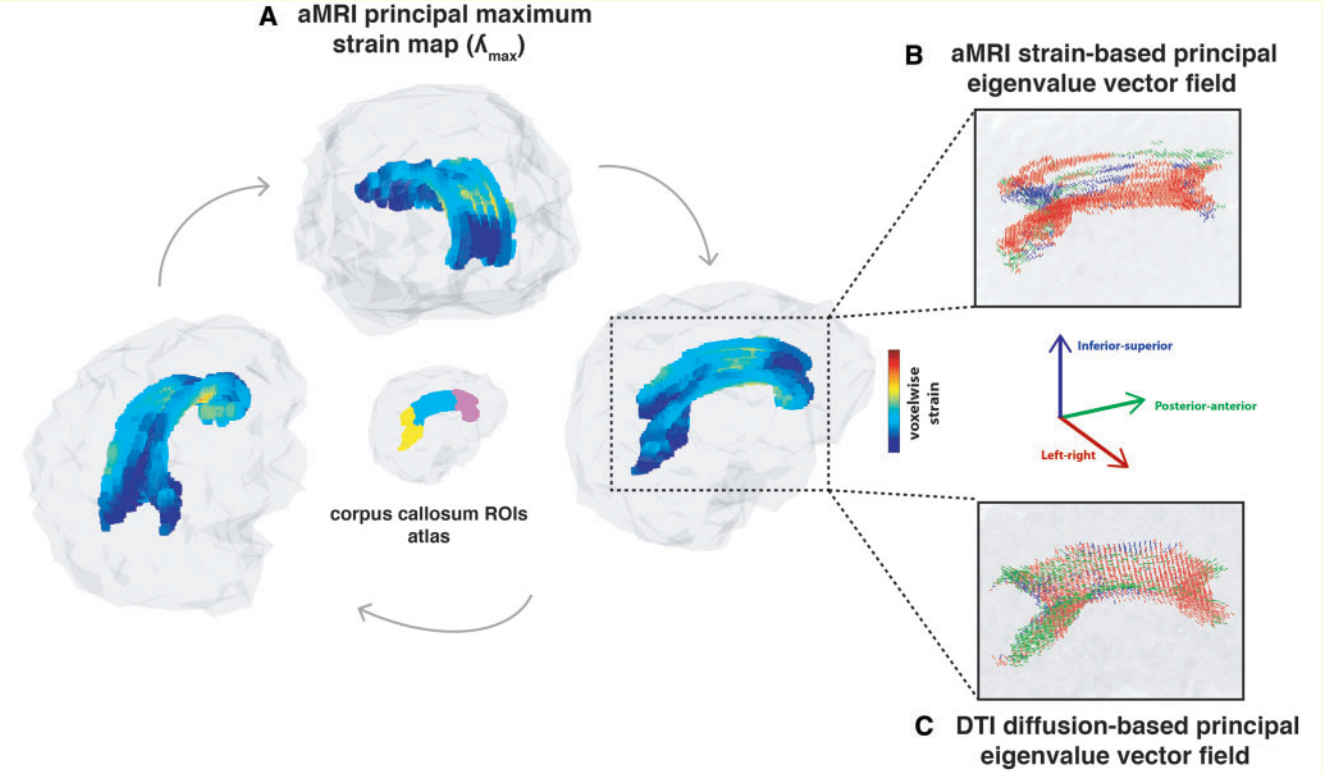

Figure 6 aMRI and DTI parameter maps of the CC. (**A**) The group-based averaged principal maximum strain (λ_{max}) map computed using aMRI, masked for the CC. The images were aligned in common space, averaged and overlaid onto the whole brain, for visual purpose only. (**B**) The voxelwise direction-weighted vector (V_1) for the principal maximum strain eigenvalue, masked for the CC, in a single representative subject. (**C**) The voxelwise direction-weighted vector (V_1) for the principal diffusion-based eigenvalue, masked for the CC, in a single representative subject, acquired form DTI. The normalized vectors in (**B**) and (**C**) are coloured based on the primary direction, showing the left–right (red), inferior–superior (blue) and posterior–anterior (green) axes. (**B**) and (**C**) provide preliminary evidence that fibre strain may follow the orientation of fibres within the white matter.

diffused axonal injury within the genu and splenium longitudinally.

Existing literature from finite element modelling of head impacts support these findings in showing that the CC is relatively tethered by the anatomy of the falx cerebri (Hernandez *et al.*, 2019), which may affect the direct transfer of rotational forces to the tissues, and induce more shearing injury of the WM fibre tract. Although the central attachment of the falx may provide some structural stability, differences in fibre compositions (i.e. differences in the number of crossing fibres per region) and other anatomical attachments along the tract may contribute to differences in strain across the fibre tract. Heterogeneity in tissue stiffness along surrounding structures like the falx cerebri may also contribute to these observed differences in λ_{max}. This is supported by findings in Hernandez *et al.* (2019), who showed that increasing the stiffness of the falx cerebri structure resulted in greater resultant strain on the CC upon impact, which emphasized the nature of the relationship between structure, tissue mechanics and possible resultant injury of the WM tract.

It is known that strain is a function of both the tissue property and the kinematic characteristics of the loading events (Beckwith *et al.*, 2018) on the brain. In addition to possible differences in tissue mechanical properties along the CC, it is possible that group differences in impact kinematics (see Supplementary Table 3) also contributed to the observed microstructural changes in WM integrity of the CC. Findings from Zhao *et al.* (2016) showed that rotational accelerations along the axes of the brain can result in a greater injury to the genu and splenium, compared to the body of the CC. The authors suggested that these differences were due to the varying degrees of motion that such impacts would induce within the falx cerebri membrane, which in turn would generate greater strain along the direction of the CC fibre tracts. It is therefore likely that group differences in WM integrity of the CC are a product of both the type and frequency of impacts that were sustained by athletes from the *HIGH* group and possible differences in the injury susceptibility of different regions along the CC fibre tract and their ability to tolerate structural deformations.

Limitations

There are a few notable limitations in this study. First, no concrete behavioural data were acquired for the athletes over time, leaving it unknown whether changes in integrity of the CC throughout the season are related to changes in behavioural outcomes. Future design may incorporate a more comprehensive behavioural tests battery such as the one presented in Nelson *et al.* (2013), in order to improve our understanding of microstructural changes along the CC and possible behavioural consequences. Second, as in with most neuroimaging designs, our findings are limited by the smaller sample size used for the *LOW* and *HIGH* exposure groups (<20 subjects), which may have decreased our statistical power and limits the generalization of our results to the broader population. Although possible day-to-day variability in DTI parameters could have biased our longitudinal results, this is unlikely to affect our findings given that previous DTI literature has shown that the reproducibility of FA over time is consistent enough (Farrell *et al.*, 2007) to allow for tracking and quantification of small longitudinal changes in subjects from experimental groups. Moreover, possible day-to-day variations due to changes in fitness over time, or other factors related to studying student-athletes, were controlled in part by the use of the *LOW* exposure group which showed no changes in FA over the course of the season and the recovery period. Future studies may also attempt to recruit a larger proportion of offensive and defensive linemen given that these positions are known to sustain a greater number of impacts to the head per-session (Crisco *et al.*, 2010, 2012).

This study is the first to leverage information from aMRI to derive strain (and indirectly, stiffness) information along the CC, as a way to inform DTI findings based on possible differences in tissue mechanics. Although the aMRI acquisition is currently limited to the acquisition of a stack of 2D slices, the post-processing analysis implemented in this study allowed for 3D reconstruction of the amplified images normalized to the heartbeat, as a way to analyse deformation fields in all directions based on the periodic cardiac-impulse function. Although tissue strain along the CC was derived from the displacement of sub-voxel motion based on the periodic physiological (cardiac) pulsation, previous research using magnetic resonance elastography has shown that viscoelastic measurements of brain tissue mechanics are dependent on the direction of the external load applied (Murphy *et al.*, 2017). Thus, this approach may be biased in part by the natural upward pulsation of the force from the heartbeat. Future research combining aMRI and magnetic resonance elastography may help to overcome this limitation, as a way to normalize the cardiac input function and provide better estimates of the brain's biomechanical response to external and physiological global forces.

Lastly, helmet accelerometers were used in this study to separate players based on a normalized index for the frequency of head impacts sustained on a per-session basis. Although this was done to bypass issues with missing data, future improvement of the helmet-based technology may allow one to limit this effect. The exposure profiles characterized for each athlete may also have been biased by other non-football related impacts, such as from players dropping their helmets on the field. However, this effect was constrained in part by using student spotters at each data collection session and retrospectively cleaning the data to delete false impacts.

Conclusion

Despite these limitations, this study design is the first to integrate novel information from aMRI as a way to provide a mechanistic explanation for the origins of microstructural differences in WM integrity due to exposure to sub-concussive impacts identified using DTI. Decreases in FA within the anterior and posterior regions of the CC were specific to players sustaining more frequent impacts to the head, indicating that this fibre tract may be vulnerable to higher rates of sub-concussive collisions sustained during the season. Using aMRI, a possible mechanism based on region-specific differences in tissue mechanics was proposed as a way to better understand differences in injury susceptibility across sections of the fibre tract.

Moving forward, combining DTI and aMRI may improve finite modelling of head impacts, as no current consensus exists in terms of the brain's material properties (van Dommelen *et al.*, 2010). Multi-modal designs such as the one proposed in this study may provide a quantitative infrastructure to study the possible consequences associated with repeated exposure to head impacts in American football players, and understand the effects of microstructural injury on brain health. Moreover, these findings emphasize the need to implement coaching practices designed to monitor and reduce exposure to head impacts during the season, in an effort to minimize possible changes in WM integrity of the brain and other possible secondary impairments that may develop from long-term exposure to sub-concussive impacts.

Supplementary material

Supplementary material is available at *Brain Communications* online.

Acknowledgements

We would like to thank Mr. Don Brien and Mrs. Janet Mirtle-Stroman for their dedication and willingness to help with data collection. The authors would like to acknowledge

Mr. Boris Baker for his help with collecting the helmet accelerometer data, along with the Queen's football program (Kingston, ON, Canada), for their participation in this research project. We are also grateful to Dr. David Dubowitz (School of Medical and Health Sciences, New Zealand) for his guidance on the imaging methods. Finally, we would like to thank Artaflex Inc. for providing the gForce Tracker equipment.

Funding

This work was supported by the Southeastern Ontario Academic Medical Organization (SEAMO) and The University of Auckland Faculty Research Development Fund strategic initiative fund. A.A.C would also like to acknowledge funding from the Ontario Graduate scholarship and the Globalink Research Award from Mitacs (ON, Canada).

Competing interests

The authors report no competing interests.

References

Aboitiz F, Scheibel AB, Fisher RS, Zaidel E. Fiber composition of the human corpus callosum. Brain Res 1992; 598: 143–53.

Adams AL, Kuijf HJ, Viergever MA, Luijten PR, Zwanenburg J. Quantifying cardiac-induced brain tissue expansion using DENSE. NMR Biomed 2019; 32: e4050.

Aletras AH, Ding S, Balaban RS, Wen H. DENSE: Displacement encoding with stimulated echoes in cardiac functional MRI. J Magn Reson 1999; 137: 247–52.

Andersson JLR, Jenkinson M, Smith S, Non-linear registration aka Spatial normalisation FMRIB Technical Report TR07JA2. In Pract. 2007: 22. Available from: http://fmrib.medsci.ox.ac.uk/analysis/techrep/tr07ja2/tr07ja2.pdf

Andersson JLR, Skare S, Ashburner J. How to correct susceptibility distortions in spin-echo echo-planar images: application to diffusion tensor imaging. Neuroimage 2003; 20: 870–88.

Asken BM, Sullan MJ, DeKosky ST, Jaffee MS, Bauer RM. Research gaps and controversies in chronic traumatic encephalopathy: a review. JAMA Neurol 2017; 74: 1255.

Basser PJ, Mattiello J, LeBihan D. MR diffusion tensor spectroscopy and imaging. Biophys J 1994; 66: 259–67.

Baugh CM, Stamm JM, Riley DO, Gavett BE, Shenton ME, Lin A, et al. Chronic traumatic encephalopathy: neurodegeneration following repetitive concussive and subconcussive brain trauma. Brain Imaging Behav 2012; 6: 244–54.

Bazarian J, Zhu T, Zhong J, Janigro D, Rozen E, Roberts A, et al. Persistent, long-term cerebral white matter changes after sports-related repetitive head impacts. PLoS One 2014; 9: 1–12.

Beaulieu C. The basis of anisotropic water diffusion in the nervous system—a technical review. NMR Biomed 2002; 15: 435–55.

Beckwith JG, Zhao W, Ji S, Ajamil AG, Bolander RP, Chu JJ, et al. Estimated brain tissue response following impacts associated with and without diagnosed concussion. Ann Biomed Eng 2018; 46: 819–30.

Broglio SP, Williams R, Rettmann A, Moore B, Eckner JT, Meehan S. No seasonal changes in cognitive functioning among high school football athletes: implementation of a novel electrophysiological measure and standard clinical measures. Clin J Sport Med 2018; 28: 130–8.

Browne KD, Chen X-H, Meaney DF, Smith DH. Mild traumatic brain injury and diffuse axonal injury in swine. J Neurotrauma 2011; 28: 1747–55.

Caccese JB, Dewolf RM, Kaminski TW, Broglio SP, Mcallister TW, Mccrea M, et al. Estimated age of first exposure to American football and neurocognitive performance amongst NCAA male student-athletes: a cohort study. Sports Med 2019; 49: 477–87.

Campbell KR, Warnica MJ, Levine IC, Brooks JS, Laing AC, Burkhart TA, et al. Laboratory evaluation of the gForce Tracker^{TM}, a head impact kinematic measuring device for use in football helmets. Ann Biomed Eng 2016; 44: 1246–56.

Champagne AA, Coverdale NS, Nashed JY, Fernandez-Ruiz J, Cook DJ. Resting CMRO 2 fluctuations show persistent network hyperconnectivity following exposure to sub-concussive collisions. NeuroImage Clin 2019; 22: 101753.

Chappell MH, Uluğ AM, Zhang L, Heitger MH, Jordan BD, Zimmerman RD, et al. Distribution of microstructural damage in the brains of professional boxers: a diffusion MRI study. J Magn Reson Imaging 2006; 24: 537–42.

Chun IY, Mao X, Breedlove EL, Leverenz LJ, Nauman EA, Talavage TM. DTI detection of longitudinal WM abnormalities due to accumulated head impacts. Dev Neuropsychol 2015; 40: 92–7.

Churchill NW, Hutchison MG, Di Battista AP, Graham SJ, Schweizer TA. Structural, functional, and metabolic brain markers differentiate collision versus contact and non-contact athletes. Front Neurol 2017; 8: 1–11.

Cookinham B, Swank C. Concussion history and career status influence sports concussion assessment tool (SCAT-3) performance in elite football players. Neurology 2018; 91: S5.3.

Cox R. AFNI: software for analysis and visualization of functional magnetic resonance neuroimages. Comput Biomed Res 1996; 29: 162–73.

Cox RW, Chen G, Glen DR, Reynolds RC, Taylor PA. FMRI clustering in AFNI: False-positive rates redux. Brain Connect 2017; 7: 152–71.

Crisco JJ, Fiore R, Beckwith JG, Chu JJ, Brolinson GP, Duma S, et al. Frequency and location of head impact exposures in individual collegiate football players. J Athl Train 2010; 45: 549–59.

Crisco JJ, Wilcox BJ, Machan JT, McAllister TW, Duhaime AC, Duma SM, et al. Magnitude of head impact exposures in individual collegiate football players. J Appl Biomech 2012; 28: 174–83.

Cubon VA, Putukian M, Boyer C, Dettwiler A. A diffusion tensor imaging study on the white matter skeleton in individuals with sports-related concussion. J Neurotrauma 2011; 28: 189–201.

Deshpande SK, Hasegawa RB, Rabinowitz AR, Whyte J, Roan CL, Tabatabaei A, et al. Association of playing high school football with cognition and mental health later in life. JAMA Neurol 2017; 74: 909–18.

Eucker SA, Smith C, Ralston J, Friess SH, Margulies SS. Physiological and histopathological responses following closed rotational head injury depend on direction of head motion. Exp Neurol 2011; 227: 79–88.

Farrell JAD, Landman BA, Jones CK, Smith SA, Prince JL, Van Zijl PCM, et al. Effects of signal-to-noise ratio on the accuracy and reproducibility of diffusion tensor imaging-derived fractional anisotropy, mean diffusivity, and principal eigenvector measurements at 1.5T. J Magn Reson Imaging 2007; 26: 756.

Finn ES, Shen X, Scheinost D, Rosenberg MD, Huang J, Chun MM, et al. Functional connectome fingerprinting: Identifying individuals using patterns of brain connectivity. Nat Neurosci 2015; 18: 1664–71.

Gajawelli N, Lao Y, Apuzzo MLJ, Romano R, Liu C, Tsao S, et al. Neuroimaging changes in the brain in contact versus noncontact sport athletes using diffusion tensor imaging. World Neurosurg 2013; 80: 824–8.

Hart J, Kraut MA, Womack KB, Strain J, Didehbani N, Bartz E, et al. Neuroimaging of cognitive dysfunction and depression in aging retired National Football League players: a cross-sectional study. JAMA Neurol 2013; 70: 326–35.

Hernandez F, Giordano C, Goubran M, Parivash S, Grant G, Zeineh M, et al. Lateral impacts correlate with falx cerebri displacement and corpus callosum trauma in sports-related concussions. Biomech Model Mechanobiol 2019: 1–19.

Herweh C, Hess K, Meyding-Lamadé U, Bartsch AJ, Stippich C, Jost J, et al. Reduced white matter integrity in amateur boxers. Neuroradiology 2016; 58: 911–20.

Holdsworth SJ, Rahimi MS, Ni WW, Zaharchuk G, Moseley ME. Amplified magnetic resonance imaging (aMRI). Magn Reson Med 2016; 75: 2245.

Hua K, Zhang J, Wakana S, Jiang H, Li X, Reich DS, et al. Tract probability maps in stereotaxic spaces: analyses of white matter anatomy and tract-specific quantification. Neuroimage 2008; 39: 336–47.

Jenkinson M, Bannister P, Brady M, Smith S. Improved optimization for the robust and accurate linear registration and motion correction of brain images. Neuroimage 2002; 17: 825–41.

Jenkinson M, Beckmann CF, Behrens TEJ, Woolrich MW, Smith SM. FSL. Neuroimage 2012; 62: 782–90.

Jenkinson M, Smith S. A global optimisation method for robust affine registration of brain images. Med Image Anal 2001; 5: 143–56.

Jeppesen MA. Young's modulus. Am J Phys 2005; 23: 300.

Johnson B, Zhang K, Gay M, Neuberger T, Horovitz S, Hallett M, et al. Metabolic alterations in corpus callosum may compromise brain functional connectivity in MTBI patients: an 1H-MRS study. Neurosci Lett 2012; 509: 5–8.

Kuriyama AM, Nakatsuka AS, Yamamoto LG. High school football players use their helmets to tackle other players despite knowing the risks. Hawaii J Med Public Health 2017; 76: 77–81.

Ling CL, Rumpel H. MRI atlas of human white matter. Concepts Magn Reson 2006; 28A: 181.

McAllister T, McCrea M. Long-term cognitive and neuropsychiatric consequences of repetitive concussion and head-impact exposure. J Athl Train 2017; 52: 309–17.

Mcallister TW, Ford JC, Flashman LA, Maerlender A, Greenwald RM, Beckwith JG. Effect of head impacts on diffusivity measures in a cohort of collegiate contact sport athletes. Neurology 2013; 82: 63–9.

McAllister TW, Ford JC, Ji S, Beckwith JG, Flashman LA, Paulsen K, et al. Maximum principal strain and strain rate associated with concussion diagnosis correlates with changes in corpus callosum white matter indices. Ann Biomed Eng 2012; 40: 127–40.

Mihalik JP, Bell DR, Marshall SW, Guskiewicz KM. Measurement of head impacts in collegiate football players: an investigation of positional and event-type differences. Neurosurgery 2007; 61: 1229.

Murphy MC, Huston J, Ehman RL. MR elastography of the brain and its application in neurological diseases. Neuroimage 2017; 187: 176–83.

Nelson LD, Janecek JK, McCrea MA. Acute clinical recovery from sport-related concussion. Neuropsychol Rev 2013; 23: 285–99.

Schmidt JD, Pierce AF, Guskiewicz KM, Register-Mihalik JK, Pamukoff DN, Mihalik JP. Safe-play knowledge, aggression, and head-impact biomechanics in adolescent ice hockey players. J Athl Train 2016; 51: 366–72.

Smith SM, Jenkinson M, Woolrich MW, Beckmann CF, Behrens TEJ, Johansen-Berg H, et al. Advances in functional and structural MR image analysis and implementation as FSL. Neuroimage 2004; 23: S208–S219.

Stamm J, Koerte IK, Muehlmann M, Pasternak O, Bourlas AP, Baugh CM. Age at first exposure to football is associated with altered corpus callosum white matter microstructure in former professional football players. J. Neurotrauma 2015; 1776: 1–37.

Stamm JM, Bourlas AP, Baugh CM, Fritts NG, Daneshvar DH, Martin BM, et al. Age of first exposure to football and later-life cognitive impairment in former NFL players. Neurology 2015; 84: 1114.

Terem I, Ni WW, Goubran M, Rahimi MS, Zaharchuk G, Yeom KW, et al. Revealing sub-voxel motions of brain tissue using phase-based amplified MRI (aMRI). Magn Reson Med 2018; 80: 2549.

van Dommelen JAW, van der Sande TPJ, Hrapko M, Peters G. Mechanical properties of brain tissue by indentation: interregional variation. J Mech Behav Biomed Mater 2010; 3: 158–66.

Wadhwa N, Rubinstein M, Durand F, Freeman WT. Phase-based video motion processing. ACM Trans Graph 2013; 32: 1.

Wakana S, Caprihan A, Panzenboeck MM, Fallon JH, Perry M, Gollub RL, et al. Reproducibility of quantitative tractography methods applied to cerebral white matter. Neuroimage 2007; 36: 630.

Weaver AA, Danelson KA, Stitzel JD. Modeling brain injury response for rotational velocities of varying directions and magnitudes. Ann Biomed Eng 2012; 40: 2005–18.

Wilde E, McCauley S, Hunter J, Bigler E, Chu Z, Wang Z, et al. Diffusion tensor imaging of acute mild traumatic brain injury in adolescents. Neurology 2008; 70: 948–55.

Woolrich MW, Jbabdi S, Patenaude B, Chappell M, Makni S, Behrens T, et al. Bayesian analysis of neuroimaging data in FSL. Neuroimage 2009; 45: S173–S186.

World Medical Association. World Medical Association Declaration of Helsinki. Ethical principles for medical research involving human subjects. Bull World Health Organ 2001; 79: 373–4.

Zhang J, Aggarwal M, Mori S. Structural insights into the rodent CNS via diffusion tensor imaging. Trends Neurosci 2012; 35: 412–21.

Zhang L, Heier LA, Zimmerman RD, Jordan B, Uluğ AM. Diffusion anisotropy changes in the brains of professional boxers. Am J Neuroradiol 2006.

Zhao W, Ford JC, Flashman LA, McAllister T, Ji S. White matter injury susceptibility via fiber strain evaluation using whole-brain tractography. J Neurotrauma 2016.